Comments on Inorganic Chemistry
Publication details, including instructions for authors and subscription information:
http://www.informaworld.com/smpp/title~content=t713455155

Some Coordination Chemistry of Non-heme Iron Nitrosyl Complexes

Lijuan Li[a]
[a] Department of Chemistry and Biochemistry, California State University, Long Beach, CA

Online publication date: 14 September 2010

To cite this Article Li, Lijuan(2002) 'Some Coordination Chemistry of Non-heme Iron Nitrosyl Complexes', Comments on Inorganic Chemistry, 23: 5, 335 — 353
To link to this Article: DOI: 10.1080/02603590215001
URL: http://dx.doi.org/10.1080/02603590215001

Comments on Inorganic Chemistry, 23: 335–353, 2002

0260-3594/02 $12.00 + .00
DOI: 10.1080/02603590290013280

Some Coordination Chemistry of Non-heme Iron Nitrosyl Complexes

Lijuan Li
Department of Chemistry and Biochemistry, California State University, Long Beach, 1250 Bellflower Blvd., Long Beach, CA 90840-3903. Phone: (562) 985-5068, Fax: (562) 985-8557, E-mail: lli@csulb.edu

The recent realization that nitric oxide is a biological messenger in many physiological processes has brought about a renewed interest in its chemistry, particularly its iron complexes that are central to the role of nitric oxide in the body. Spectroscopic evidence would appear to implicate species of "$Fe(NO)_2^+$" type, so called non-heme iron nitrosyls, in a variety of processes ranging from polymerization, carcinogenesis, to nitric oxide stores. This article describes two types of coordination chemistry of non-heme iron nitrosyl complexes. One type is the interactions of $Fe(NO)_2$ with a series of substituted imidazoles, benzimidazoles and histidines, and the other is the coordination of a tetracyanoethylene group and a variety of phosphine and phosphite ligands to the $Fe(NO)_2$ moiety. A combination of different techniques, such as NMR, IR, EPR, electrochemistry, and X-ray crystallography, in stydying the structures and dynamics of these systems are discussed.

Keywords: non-heme iron, iron dinitrosyls, nitrosyls, iron nitrosyls, EPR, NMR, X-ray structures, phosphines, phosphites, tetracyanoethylene, imidazoles, histidine

INTRODUCTION

Recent investigations have demonstrated that nitric oxide plays key roles in many diverse cellular functions, such as in controlling blood pressure, preventing platelet aggregation, acting as biological messengers and immune

Address correspondence to Lijuan Li, Department of Chemistry and Biochemistry, California State University, 1250 Bellflower Blvd., Long Beach, CA 90840-3903. E-mail: lli@csulb.edu.

system cytotoxic agents, and being involved in memory storage.[1] These discoveries have stimulated intense interest in metal-nitrosyl complexes, especially those that mimic the structures of biological active metal complexes. Very recently, *Chemical Reviews* has dedicated a special issue on nitric oxide chemistry.[2]

One of the first clues that the immune system utilizes NO to combat pathogens came from electron paramagnetic resonance (EPR) studies in cells showing the formation of $Cys_2Fe(NO)_2$.[3] It has been proposed that NO may react directly with ferrodoxin proteins such as aconitase, an enzyme containing a 4Fe-4S cluster that catalyses the isomerization of citrate to isocitrate in the citric acid cycle, destroying the iron-sulfur cluster which results in the loss of enzymatic activity. Extensive EPR studies have identified non-heme iron-nitrosyl complexes as products after biosynthetic evolution of NO *in vitro*.[2,4] Muller *et al*.[5] and other groups[6,7] have also reported evidence that nitric oxide stores as non-heme iron-nitrosyl complexes. Recently, a light-sensitive nitrile hydratase from *Rhodococuss* sp. N771 was found to have a NO molecule bound to the non-heme iron center.[8] This enzyme is activated upon irradiation, followed by the release of NO from the iron center.

These non-heme iron-nitrosyl complexes are paramagnetic complexes of the type "$Fe(NO)_2$," more commonly referred to as "$g = 2.03$" complexes because of their characteristic isotropic g-factor from the EPR spectroscopic studies. Lee *et al*. identified three types of EPR-active non-heme iron-nitrosyl complexes in mammalian ferritins, which have been attributed to iron-nitrosyl complexes with imidazole groups of histidine, thiol groups of cysteine, and carboxylate groups of aspartate and glutamate, respectively.[9] To this day, a large number of compounds of the form $Fe^{I}(NO)_2(L)_2$ in which the ligand L is derived from amino acids, peptides, and proteins, has been detected by EPR spectroscopy, but has not been isolated.[10,11,12] The trend has been to detect the presence of these compounds rather than isolate them, because the isolation and structural determination of these compounds by means other than IR and EPR are both extremely tedious and difficult, and to our knowledge none are known.

The majority of known $L_2Fe(NO)_2$ compounds contain P and S donor ligands.[13,14] In searching literature precedent for isolated iron-nitrosyl with nitrogen donor ligands and/or imidazole types of ligands coordinated to iron, only two examples were found: a tetrahedral compound of $[(DAD)Fe(NO)_2]$, (DAD = diazadiene)[15] and a complex with the 3,5-dimethylpyrazolyl iron dinitrosyl dimer, $[(N_2C_5H_7)Fe(NO)_2]_2$.[16] More recently, Rettig *et al*. published a polymeric iron(II)-imidazole complex $[Fe(Im)_4]_n$ involving octahedral and tetrahedral iron centers.[17] In the effort of modeling non-heme iron enzymes, Hagadorn *et al*. recently reported the X-ray crystal structure of iron with 1-methylimidazole and carboxylate 2,6-dimethylbenzoate ligands, $(Mes_2\text{-}ArCO_2)_2Fe(1\text{-}MeIm)_2$.[18]

From the chemistry point of view, the catalytic activity of iron dinitrosyl complexes has been known for decades, and has been the focus of several reports, including studies of the catalytic activity of these complexes in the cyclodimerization of dienes, and in the polymerization of styrene and acrylonitrile.[19,20,21] In 1987, Gadd and coworkers proposed that the dimerization of butadiene might occur *via* the intermediacy of $Fe(NO)_2(\eta^2\text{-}C_4H_8)(\eta^4\text{-}C_4H_8)$, where one nitrosyl ligand is linear and the other is bent.[22] These olefin-bound metal nitrosyls were not stable and decomposed at temperatures as low as $-50°C$. Although π-bound-olefin iron dinitrosyl intermediates have been proposed in the catalytic action of iron nitrosyls, most of these complexes have been only characterized by use of *in situ* spectroscopic techniques, such as EPR spectroscopy and IR spectroscopy. The catalytic activities are summarized[23] and the electronic structures of these compounds are rationalized as 17 electron complexes with a d^9 electron configuration.[24,25] Recently, Postel *et al.* found that iron nitrosyls can activate molecular oxygen in the presence of bidentate phosphine ligands[26] and nitrogen ligands.[27]

In this article, we will summarize the chemistry of two types of iron dinitrosyl complexes prepared in our laboratory. One is the biomimic non-heme, non-sulfur iron-nitrosyl compounds, $Fe(NO)_2(1\text{-MeIm})_2$, **1**, which will help us to gain insight into the structures of non-heme iron nitrosyls and to establish the important relationship between structures and functions of these molecules in biological systems. Another one is a series of $Fe(NO)_2(PR_3)(\eta^2\text{-TCNE})$ complexes, where $PR_3 = PPh_3$, **2**,[28] $P(OCH_3)_3$, **3**, $P(n\text{-Bu})_3$, **4**, PMe_2Ph, **5**, and PEt_2Ph, **6**.[29] We will describe the syntheses, structure, dynamics, and electrochemical behavior.

INTERACTION OF NON-HEME IRON NITROSYL WITH IMIDAZOLE LIGANDS

EPR has been one of the most commonly employed techniques for the characterization of non-heme iron-nitrosyl complexes in biological systems. Thus, the reaction of $Fe(NO)_2(CO)_2$ and 1-methylimidazole (1-MeIm) was first studied by EPR to establish the validity of using this ligand as the biomimic model. At 240 K, the starting material, $Fe(NO)_2(CO)_2$, produced a broad singlet with $g = 2.0275$ and $\Delta H_{pp} = 18.5$ G as seen in Figure 1a. Upon the addition of 1-MeIm, a new set of signals overlapping with the broad singlet was observed in about 15 minutes (Figure 1b). This nine line spectrum (Figure 1c) shows a g value of 2.0151, which is typical for iron dinitrosyl radicals with an unpaired electron localized on the Fe as discussed in our previous work.[30] Simulation (Figure 1d) gave rise to two sets of equivalent nitrogens (^{14}N, $I = 1$) with hyperfine coupling constants of 3.60 G and 3.90 G, respectively. The hyperfine structure is due to coupling of two equivalent ^{14}N

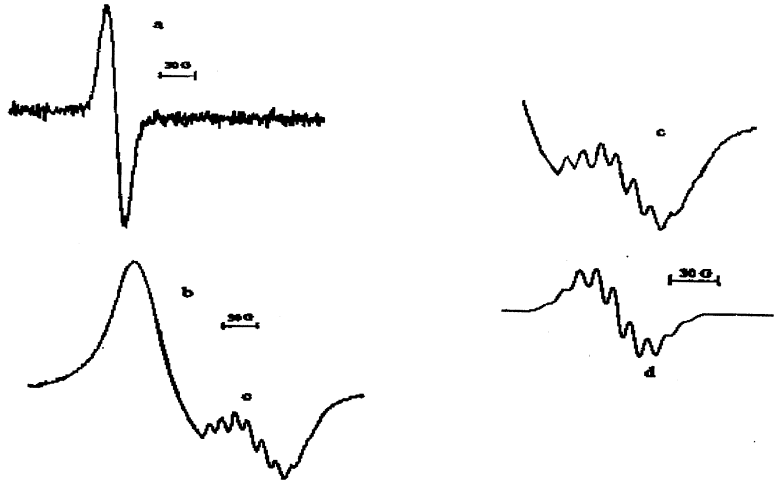

FIGURE 1 First derivative EPR spectra of the reaction of $Fe(NO)_2(CO)_2$ with 1-MeIm in diethylether. (a) EPR spectrum of $[Fe(NO)_2(CO)_2]^+$ ($g = 2.0275$) at room temperature. (b) EPR spectrum reveals new radical ($g = 2.0151$) formation (9-line) after the addition of 1-MeIm at room temperature. (c) Experimental expansion of the 9-line EPR spectrum at 240 K. (d) Computer simulation with $a_{N1} = 3.6$ G and $a_{N2} = 3.9$ G for the signal of $[Fe(NO)_2(1\text{-MeIm})_2)]^+$.

nuclei from the nitrosyls and two equivalent ^{14}N nuclei from the 1-MeIm, yielding a structure of $Fe(NO)_2(1\text{-MeIm})_2^+$, shown in Scheme 1.

The EPR signals arising from the intermediates disappeared over a period of time and the crystalline compound, $Fe(NO)_2(1\text{-MeIm})_2$, **1**, was isolated

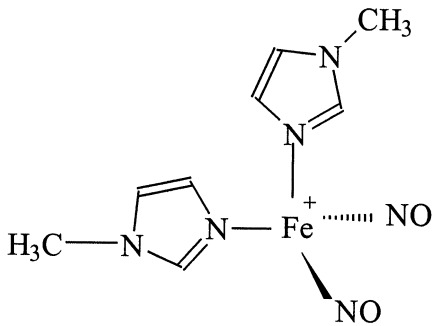

SCHEME 1 Molecular structures of $[Fe(NO)_2(1\text{-MeIm})_2]^+$.

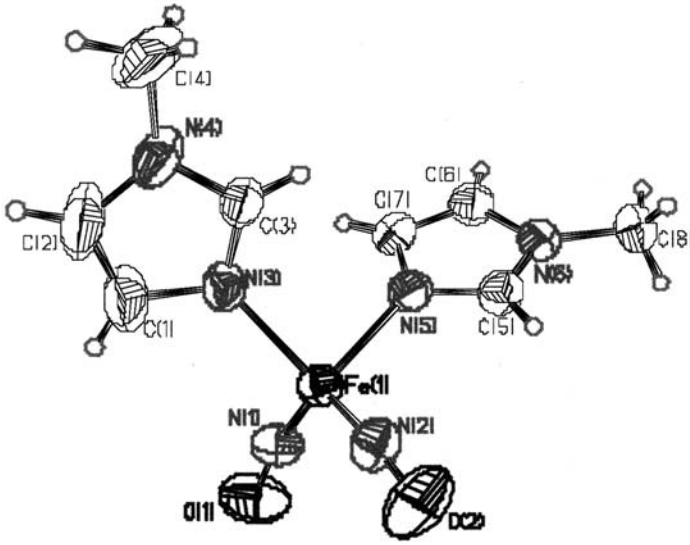

FIGURE 2 The X-ray structure of $Fe(NO)_2(1\text{-MeIm})_2$, showing the atomic numbering scheme. Anisotropic thermal displacement ellipsoids are shown at the 50% probability level. From ref. 31.

from the solution. Single crystals of **1** suitable for X-ray analysis were obtained from diethyl ether. The X-ray crystal structure[31] of $Fe(NO)_2(1\text{-MeIm})_2$ is shown in Figure 2. Compound $Fe(NO)_2(1\text{-MeIm})_2$ is monoclinic and crystallizes in a $C_{2/c}$ space group, with 8 molecules per unit cell. The crystal packing is shown in Figure 3. The complex is pseudo-tetrahedral with a d^{10} iron center. The nitrosyl groups are linear with Fe-N-O angles of 167.5(3)° and 170.1(3)°, and are displaced at the N(NO)-Fe-N(Im) angles of 111.28(13)° and 107.78(13)° away from the imidazole ligands. The Fe-N(1) and Fe-N(2) bond distances of the nitrosyls are 1.648(3) and 1.650(3) Å, respectively. The Fe-N-O groups are bent symmetrically, with a O-Fe-O angle of 107.3° as compared with the N(NO)-Fe-N(NO) angle of 116.6°. This is considered an "attracto" conformation because the N-M-N bond angle is less than 130° and the two oxygen atoms bend towards each other. "Attracto" conformations generally favor first row transition-metal dinitrosyls containing ligands that are good π-acceptors.[32] The Fe-N(3) and Fe-N(5) bond distances of the 1-methylimidazole are 2.048(3) and 2.044(3) Å, respectively. The horizontal plane through each 1-methylimidazole ligand is skewed 106.7° away from the other.

$Fe(NO)_2(1\text{-MeIm})_2$ was characterized by FT-IR and NMR spectroscopic methods. Infrared spectroscopy of $Fe(NO)_2(1\text{-MeIm})_2$ revealed NO stretching

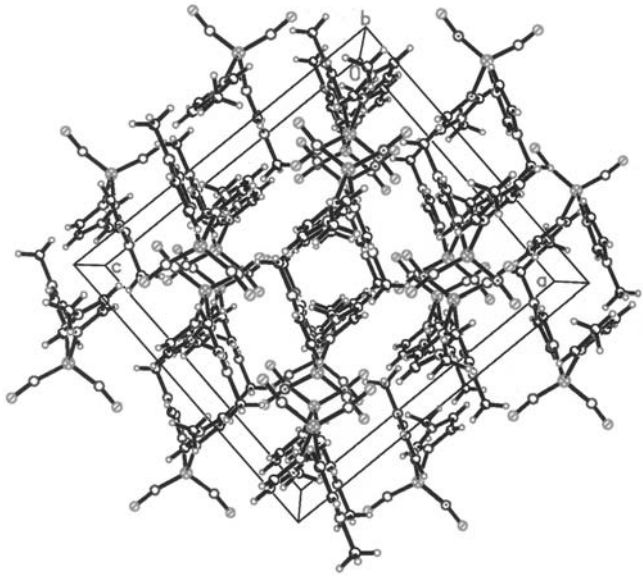

FIGURE 3 The crystal packing diagram of $Fe(NO)_2(1\text{-MeIm})_2$.

frequencies at 1673 and 1616 cm^{-1}, which fall into the region of linear nitrosyls. The addition of the imidazole ligand resulted in lowering the ν_{NO} by approximately 140 cm^{-1}, suggesting that 1-MeIm acts as a strong σ-donor rather than a π-acceptor. The ^{1}H and ^{13}C NMR spectra were measured by reacting two equivalents of ligand with one equivalent of $Fe(NO)_2(CO)_2$ in deuterated methanol. After gas evolution subsided, an aliquot was removed and placed in an NMR tube where the sample was degassed by freeze-pump-thaw procedures and then flame–sealed under vacuum. The proton spectrum for $Fe(NO)_2(1\text{-MeIm})_2$ shows a mixture of 1-MeIm and $Fe(NO)_2(1\text{-MeIm})_2$ in solution. The broad signal at 8.79 ppm is attributed to H2 and H4 of $Fe(NO)_2$-$(1\text{-MeIm})_2$. It is believed that the resonances of H2 and H4 are similar, and with line broadening, only one broad signal is observed. The 1-MeIm ligand acts as an electron donor, and so the protons of H2 and H4 are deshielded upon complexation with the iron and are shifted further downfield with respect to the free 1-MeIm molecule. The signal at 4.99 ppm is assigned to H5, which is not subjected to any deshielding by complexation. The broad peak at 3.97 ppm is assigned to the CH_3 group. The peaks at 7.68, 7.10, 6.87, and 3.68 ppm are assigned to H2, H4, H5, and CH_3 of the free 1-MeIm ligand, respectively.

The ^{13}C spectrum also reveals a mixture of 1-MeIm and $Fe(NO)_2$-$(1\text{-MeIm})_2$ in solution. The small signals at 226.2 and 225.6 ppm are attributed

TABLE 1 List of EPR Data of the Cationic Radicals for the Reaction of $Fe(NO)_2(CO)_2$ with Substituted Imidazoles, Benzimidazoles and L-histidine Measured at 240 K[a]

Cationic radicals	No. of lines	g-value	Preliminary a_N value (G)
$Fe(NO)_2(1\text{-MeIm})_2^{+}$[b]	9	2.0151	$a_{N1} = 3.60$; $a_{N2} = 3.90$
$Fe(NO)_2(4\text{-MeIm})_2^{+}$	9	2.0338	$a_{N1} = 2.33$; $a_{N2} = 2.64$
$Fe(NO)_2(Im)_2^{+}$	9	2.0337	$a_{N1} = 2.28$; $a_{N2} = 2.44$
$Fe(NO)_2(BenzIm)_2^{+}$	9	2.0341	$a_{N1} = 1.97$; $a_{N2} = 2.12$
$Fe(NO)_2(ME_2BenzIm)_2^{+}$	9	2.0352	$a_{N1} = 1.88$; $a_{N2} = 2.04$
$Fe(NO)_2(L\text{-Histidine})_2^{+}$	9	2.0222	$a_{N1} = 2.66$; $a_{N2} = 3.01$

[a]Measured in THF solution;
[b]Measured in diethyl ether solution.

to either C2 or C4 carbons. Again, these atoms are affected by the deshielding that occurs upon complexation. Definitive assignment of the chemical shifts of the two carbon atoms is not made. The peak at 143.4 ppm is assigned to the C5 carbon and the broad peak at 38.3 ppm is attributed to the CH_3 carbon. The resonance peaks at 143.6, 134.2, 123.1, and 34.2 ppm arise from the C2, C4, C5 and CH_3 carbons of the free 1-MeIm ligand, respectively.

In order to mimic biological systems, the reaction of $Fe(NO)_2(CO)_2$ with 4-methyl imidazole (4-MeIm), imidazole (Im), benzimidazole (BenzIm), 5,6-dimetheylbenzimidazole (Me_2BenzIm), and L-histidine were also investigated by EPR spectroscopy. Table 1 lists the EPR parameters measured at 240 K in solution. The g-values for the imidazole and substituted imidazole radicals fall in the range of 2.0151 to 2.0338 and a_N in the range of 2.28 to 3.90 G. For benzimidazole and substituted benzimidazole, the g-values are slightly higher (2.0341–2.0352) while the a_N values are smaller (1.88 G–2.12 G). For L-histidine, both g value (2.0222) and hyperfine couplings (2.66 G and 3.01 G) fall in the range of substituted imidazoles. These EPR spectra are obviously the same as previously observed ones by directly reacting a Fe^{2+} salt and gaseous NO with imidazole, N-ethylimidazole or benzimidazole, which was reported as a nine hyperfine component spaced about 2.5 G apart and at a g_{av} factor of 2.027.[33]

FT-IR investigations showed that upon addition of the imidazole ligands to $Fe(NO)_2(CO)_2$, the ν_{NO}'s were lowered by approximately 140 wavenumbers and no carbonyl stretching frequencies were observed. This indicates that two Im ligands had replaced the two CO ligands. The nitrosyls fall into the region of 1650–1940 cm^{-1}, indicating they are linear. Table 2 lists the NO stretching frequencies observed for these complexes. Addition of 1-MeIm shifted the IR stretching frequencies of nitrosyls from 1810 and 1767 cm^{-1} [ν_{NO} for $Fe(NO)_2(CO)_2$] to 1673 and 1616 cm^{-1}, suggesting that

TABLE 2 Nitrosyl Stretching Frequencies for some of the Complexes

Compound	ν_{NO} (cm^{-1})
$Fe(NO)_2(Im)_2$	1680, 1622
$Fe(NO)_2(1\text{-MeIm})_2$	1673, 1616
$Fe(NO)_2(4\text{-MeIm})_2$	1677, 1620
$Fe(NO)_2(BenzIm)_2$	1682, 1625
$Fe(NO)_2(Me_2BenzIm)_2$	1683, 1625

1-MeIm acts as a strong σ-donor. To explain the trend in the IR stretching frequencies, EHMO calculations were made.[34] An interaction diagram shows the energy difference between the LUMO and HOMO of the 1-MeIm fragment to be much higher than that of the $Fe(NO)_2$ fragment. In other words, the LUMO of the $Fe(NO)_2$ unit has more contribution to the overall molecular orbitals. Thus, effectively, imidazole units act as electron donors to the LUMO of $Fe(NO)_2$ fragment. The net positive charge on Fe decreases when the 1-MeIm ligands replace the CO ligands, while the negative charges on the nitrogens of the imidazole ligands also decrease, again inferring that the 1-MeIm ligands are donating electron density onto iron. The donation of electron density onto the iron center also results in a decrease of the positive charges on the nitrogens of the nitrosyls, which indicates the increase of the backbonding into the π* orbital of the NO ligand. This explains the weakening of the NO bond and shifting of the NO stretches.

IRON DINITROSYL COMPLEXES CONTAINING PHOSPHINE AND TCNE LIGANDS

Complexes of $Fe(NO)_2(CO)(PR_3)$, ($R = PPh_3$, OCH_3, $P(n\text{-}Bu)_3$, PMe_2Ph, PEt_2Ph), were synthesized by reacting 1:1 ratio of $Fe(NO)_2(CO)_2$ with the appropriate phosphine ligand at room temperature for 12–15 hours, and were monitored by IR and NMR spectroscopic methods. These compounds reacted rapidly with TCNE to afford the complexes $Fe(NO)_2[PR_3](\eta^2\text{-TCNE})$, ($PR_3 = PPh_3$, **2**, $P(OCH_3)_3$, **3**, $P(n\text{-}Bu)_3$, **4**, PMe_2Ph, **5**, and PEt_2Ph, **6**) in good yield. Generally, carbonyl substitution reactions are slow, requiring for overnight to replace the first carbonyl and requiring heating at 85°C for 1–2 days to replace the second carbonyl.[35] The $Fe(NO)_2(L)_2$ [$L = PR_3$, NR_3] compounds formed by reaction of $Fe(NO)_2(CO)_2$ and L have been shown to proceed by a conventional associative mechanism.[36] However, in this reaction, the substitution of CO by TCNE is completed in 1–2 hours at room temperature. Intermediates of $TCNE^-$ and $Fe(NO)_2(PPh_3)L^+$ (L maybe CO or solvent) radicals were observed using EPR upon mixing of the starting materials. Thus, the rapidity of such a substitution reaction is due to the

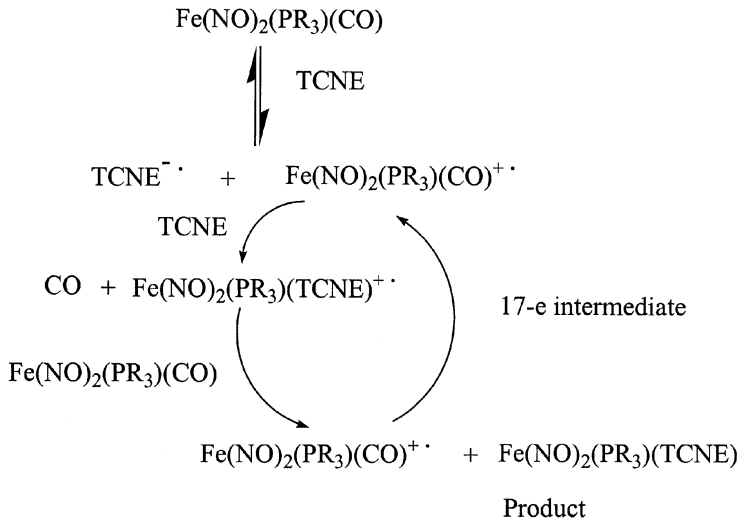

SCHEME 2 Mechanism of the reactions of $Fe(NO)_2(CO)(PPR_3)$ with TCNE showing the electron transfer autocatalytic pathway through a 17-electron intermediate.[28]

participation of free radicals. It is believed that the reaction proceed *via* an electron transfer autocatalysis mechanism, through a 17-electron paramagnetic intermediate as shown in Scheme 2.[28]

Compounds **2–6** are soluble in polar solvents such as CH_2Cl_2, THF, $(CH_3)_2CO$, CH_3CN and MeOH (but not in diethyl ether and water), however complete decomposition occurs after a few hours. When stored in the solid state at ambient temperature under an atmosphere of nitrogen similar decomposition occurs, albeit much more slowly. The rapid decomposition of these complexes in polar solvents can be rationalized in terms of a nucleophile-induced disproportionation reaction, as observed in the reaction of $[Fe(CO)_3(PPh_3)_2]^+$ and pyridine,[37] and in the conversion of $Fe(NO)_2(PPh_3)_2^+$ to $Fe(NO)_2(PPh_3)_2$.[25]

The FT-IR data for the mono-substituted products, $Fe(NO)_2(CO)(PR_3)$, the TCNE adducts, $Fe(NO)_2(PR_3)(\eta^2\text{-TCNE})$ (**2–6**), and other related complexes are listed in Table 3. The spectrum of the starting material, $Fe(NO)_2(CO)_2$, exhibits two nitrosyl stretches and two carbonyl stretches. Upon replacement of a single carbonyl moiety by a phosphite or phosphine group, the remaining CO absorbs around 1995–2018 cm^{-1}. Replacement of the second carbonyl group by TCNE gives rise to a peak $\sim 2225\,cm^{-1}$, attributable to the nitrile functionalities.

On examination of the two nitrosyl IR stretches in these complexes, a noticeable trend arises in the shifts of these peaks when carbonyl groups are

TABLE 3 List of IR Frequencies of Related Iron Dinitrosyl Complexes

Complexes	CN stretch (cm^{-1})	CO stretch(es) (cm^{-1})	NO stretches (cm^{-1})
$Fe(NO)_2(CO)_2$	–	2090; 2040	1817; 1766
$Fe(NO)_2(PPh_3)(CO)$	–	2007	1766; 1718
$Fe(NO)_2(PPh_3)(\eta^2$-TCNE), **2**	2224	–	1834; 1790
$Fe(NO)_2[P(OMe_3)](CO)$	–	2018	1770; 1722
$Fe(NO)_2[P(OMe)^3]$	2230	–	1843; 1790
(η^2-TCNE), **3**	(2233)[a]		(1843; 1797)
$Fe(NO)_2[P(n\text{-}Bu)_3](CO)$	–	(1995)	(1752; 1704)
$Fe(NO)_2[P(n\text{-}Bu)_3]$	2229	–	1828; 1778
(η^2-TCNE), **4**	(2230)		(1824; 1785)
$Fe(NO)_2[PMe_2Ph](CO)$	–	(2004)	(1754; 1708)
$Fe(NO)_2[PMe_2Ph]$	2219		1839; 1792
(η^2-TCNE), **5**	(2226)		(1830; 1786)
$Fe(NO)_2[PEt_2Ph](CO)$		(2004)	(1755; 1706)
$Fe(NO)_2[PEt_2Ph]$	2225	–	1812; 1755
(η^2-TCNE), **6**	(2231)		(1827; 1790)

[a]The numbers shown in brackets were measured in CH_2Cl_2 solution.

substituted by other ligands. The phosphorus donor increases the electron density at the iron center, which in turn enhances the back-bonding from the filled *d*-orbitals on the metal to the vacant anti-bonding orbitals of the nitrosyls, with concomitant weakening of the N≡O bond. This results in a shift of the nitrosyl stretches towards lower wavenumbers, in the region of 1700 to 1770 cm^{-1}. In contrast, the electron-withdrawing effect of TCNE reduces back-bonding, which in turn strengthens the nitrosyl bond, resulting in a shift of the two nitrosyl peaks to higher frequencies (1755 cm^{-1} and 1843 cm^{-1}). The magnitude of this high frequency shift completely compensates for the bond weakening observed on initial incorporation of the phosphine or phosphite moiety. In the meanwhile, Liaw et al. also noticed that the oxidation level of $Fe(NO)_2$ is the primary determinant of ν(NO) values; they are also highly sensitive to ancillary ligands and the distal metal influence through the bridging thiolate donor.[38]

Typically, ferrocene reacts with TCNE to form charge transfer complexes of the type $(\eta^5\text{-}C_5Me_5)_2Fe^+(TCNE)^-$, in which the cyano stretching frequency appears unchanged from free TCNE.[39] The σ-bonded TCNE (Fig. 4a) shows multiple CN absorptions owing to the effective local C_s symmetry of the coordinated TCNE.[40] The observation of only one broad cyano stretching frequency in the IR spectrum of **2–6**, in both solid state and in solution, confirms that the TCNE moiety is in fact π-bonded to the iron.

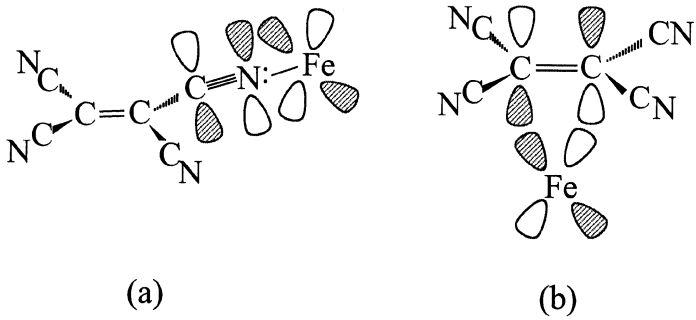

FIGURE 4 Molecular orbital illustration of the TCNE σ and π bonding to the metal. (a) TCNE σ-bond. (b) TCNE π-bond.

The cyano stretching frequency is shifted to lower wavenumbers in comparison to the corresponding stretching frequencies for free TCNE, and can be interpreted in terms of the efficient back-donation from the filled metal *d*-orbitals on iron into the vacant π^*-orbital of TCNE. This back-donation results in a weakening of the C ≡ N bond, as depicted in Figure 4b.

Using suitable single crystals grown from diethyl ether and methylene chloride, the crystal structures of **2** and **3**, were determined, as shown in Figure 5 and 6.

In both cases, the iron center exhibits distorted tetrahedral geometry and is bound to two nitrosyl groups, one phosphorus ligand and one π-bonded TCNE ligand. The two nitrosyl groups in **3** are nearly linear with angles of 175.1(7)° and 172.6(6)°, while for **2**, angles of 178.0(5)° and 165.8(5)° were observed.[28] The $Fe(NO)_2$ unit is in an *attracto* conformation in **3** with O-Fe-O and N-Fe-N angles of 116.2° and 120.9°, respectively. The average N-O distance in **3** (1.158(8) Å) is similar to the corresponding values found in **2** (1.169(7) Å)[9] and $Fe(NO)_2(CO)_2$ (1.171 Å),[41] suggesting that the electron-withdrawing effect of the TCNE moiety is sufficient to counteract the corresponding electron-donating strength of the phosphorus ligand, as compared to the $Fe(NO)_2(CO)_2$ reference.

The dihedral angle between the plane containing C(1) = C(2), that is perpendicular to the Fe-C(1)-C(2) plane and the plane containing C(1)-C(12)-N(12), and C(11)-N(11) is 15.6°. This loss of planarity presumably results from the back-donation of electron density from the metal to the alkene π^* manifold; this phenomenon is, of course, well established, especially for ligands such as C_2F_4 that possess highly electron-negative substituents.[42] The steric demands of the phosphorus ligand in **3** are manifested in the asymmetric bonding of the iron center to the ethylenic moiety. The lengthened Fe-C(2) bond (2.074(7) Å) nearest the trimethylphosphite group, relative to the related Fe-C(1) distance (2.024(6) Å) opposite

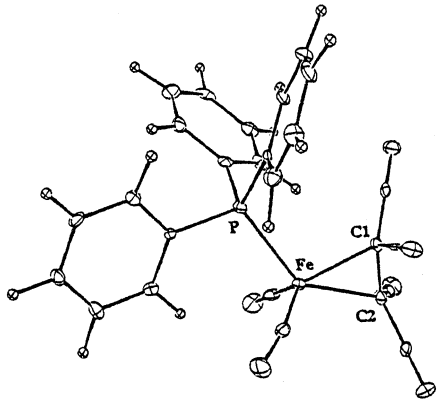

FIGURE 5 The X-ray crystal structure of $FE(NO)_2(PPh_3)(\eta^2\text{-TCNE})$. Solvent molecule diethyl ether was crystallized together with the compound and was not shown here. From ref. 28.

the phosphorus moiety, can be rationalized in terms of unfavorable steric interactions of the phosphite group with the C(21)-N(21) and C(22)-N(22) nitriles. These steric effects are enhanced in the $Fe(NO)_2(PR_3)(\eta^2\text{-TCNE})$ series when even bulkier phosphorus ligands such as R = Ph,[28] or

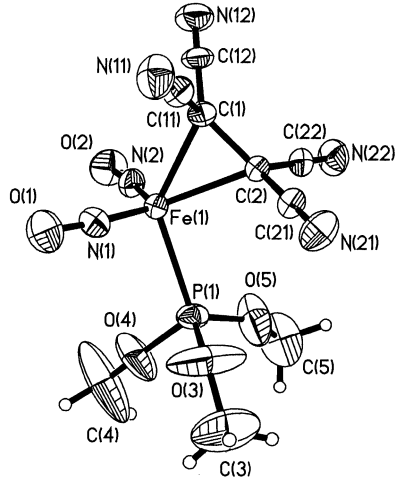

FIGURE 6 The molecular structure of $Fe(NO)_2P(OME)_3(\eta^2\text{-TCNE})$, **3**, determined by X-ray diffraction. Anisotropic thermal ellipsoids are shown at 30%. Reprinted from ref. 29, with permission from Elsevier Science.

R = cyclohexyl,[43] are employed. The relevance of steric effects in TCNE-metal complexes was also demonstrated by McGinnety and Ibers, who reported the formation of an unexpected *cis*-diphosphine adduct to Vaska's Br-compound, IrBr(CO) $(PPh_3)_2(\eta^2$-TCNE), attributable to the steric demands of the phosphine and the TCNE ligand.[44]

Complex **3** is sufficiently stable in CD_2Cl_2 in a vacuum-sealed NMR tube to allow for a detailed NMR study. The 125 MHz ^{13}C-NMR spectrum of **3** in CD_2Cl_2 at room temperature showed pairs of cyano peaks at 113.1 ppm ($J_{C\text{-}P} = 4.0$ Hz) and 113.3 ppm ($J_{C\text{-}P} = 5.6$ Hz), in addition to the expected methoxy carbon at 55.3 ppm ($J_{C\text{-}P} = 6.5$ Hz). A very weak peak at 29.0 ppm, corresponding to the ethylene carbons, was also observed. The low intensity of the aforementioned peak may be attributable to its relatively long relaxation time. Because of coordination to the iron center, the ethylene carbons are significantly shielded compared to those of free TCNE (112.6 ppm). This phenomenon was also observed in the ^{13}C NMR spectrum of **2**.[28] The crystallographic data support these observations, especially the lengthening of the C(1)-C(2) distance in the π-bonded TCNE moiety relative to free TCNE. These chemical shifts are indicative of significant sp^3-character at the olefinic carbons of the tetracyanoethylene moiety. It should also be pointed out that in $Pt(PPh_3)_2(\eta^2$-CH_3-$CF=CF_2)$, the ^{19}F NMR spectrum shows a geminal $^2J_{FF}$ coupling constant of 200 Hz, which is of the order observed in saturated fluorocarbon systems.[45] Similar trends were also observed in the Rh complex of $(C_5H_5)Rh(\eta^2$-$C_2F_4)(\eta^2$-$C_2H_4)$.[46]

The crystallographically-determined structures of **2** and **3,** as viewed down the centroid of C(1)-C(2) bond to the iron atom, are presented in Figure 7. From this perspective it is evident that **2** and **3** adopt an interesting geometry, in which two of the nitrile groups are oriented directly above the two nitrosyl ligands and are different from the others. The two sets of cyanocarbon peaks in the ^{13}C NMR spectrum at room temperature indicate that, in agreement with the solid-state structure, rotation along Fe-TCNE π-bond is restricted on the NMR time-scale.

The variable-temperature ^{13}C NMR spectra (in CD_3CN), shown in Figure 8, shows peak coalescence at about 70°C. Unfortunately, sample decomposition above 80°C prevented the acquisition of data in the fast exchange region, so a complete line-shape analysis was not possible. Nevertheless, the Gutowsky-Holm approximation yields a value for $\Delta G_{343}^{\ddagger}$ of 18.1 ± 0.5 kcal/mol.[47] This barrier is rather high compared to the published barriers for the rotation of coordinated olefins. Typically, Cramer and coworkers reported barriers for C_2H_4 rotation in the complexes $(C_5H_5)Rh(\eta^2$-$C_2H_4)_2$, $(C_5H_5)Rh(\eta^2$-$C_2H_4)(\eta^2$-$C_2F_4)$, and $(C_5H_5)Rh(\eta^2$-$C_2H_4)SO_2$ of 15.0 kcal/mol, 13.6 kcal/mol, and 12.2 kcal/mol, respectively. However, it was not possible to observe rotation about the Rh-C_2F_4 axis in $(C_5H_5)Rh(\eta^2$-$C_2H_4)(\eta^2$-$C_2F_4)$.[45] Kaneshima *et al.* have also studied the rotational processes of TCNE ligand in a series of $[Rh(RNC)_{4-n}(PPh_3)_n$-$(\eta^2$-TCNE)]X complexes, in which slowed rotation of the TCNE ligand was

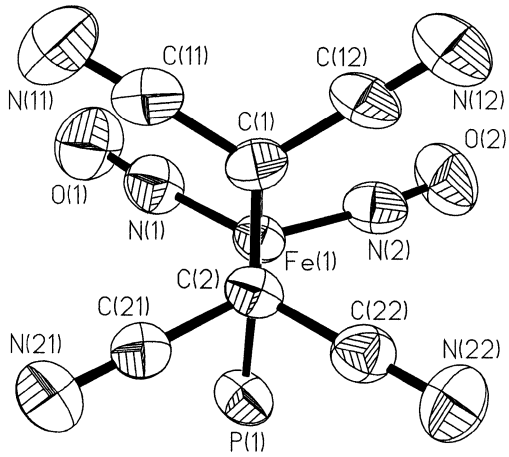

FIGURE 7 The molecular structure of **3** showing 50% thermal ellipsoids, viewed from the centroid of the C(1)-C(2) bond to the iron atom. The OCH_3 groups have been omitted for clarity. Reprinted from ref. 29. Copyright (1998), with permission from Elsevier Science.

only observed when $n = 0$; however, no barrier was obtained.[48,49] Clearly, the increased barrier to TCNE rotation is a reflection of the enhanced back-donation from metal *d*-orbitals into π^* of the alkene; a similar rationale has been proposed by Wheelock *et al*. for platinum(0) and acetylene and olefin complexes.[50] The orientation shown in Figure 6 may be a result of favorable π-orbital interactions between the $N \equiv O$ and $C \equiv N$ π-systems, which would be broken upon rotation of the TCNE group. These π-interactions may contribute in part to the observed increase in the rotational activation energy barrier, in comparison to related metal-olefin systems.

Cyclic voltammograms of the complexes **3–6** and its precursors, $Fe(NO)_2(PR_3)(CO)$, were recorded in CH_2Cl_2 containing 0.1 M electrolyte, and the data are collected in Table 4. The compounds, $Fe(NO)_2(PR_3)(CO)$, demonstrated a quasi-reversible reduction potential E° from -1.96 V to -2.15 V with large peak-to-peak separations. Upon replacement of the carbonyl by TCNE, the reduction becomes irreversible. Table 4 lists the reduction potentials, E_{pc}, of complexes **3, 4, 5** and **6** at a scan rate of 100 mV/s. This reduction has no corresponding oxidation peak, even at a scan rate of 1000 mV/s, which indicates that the reduction is chemically irreversible at room temperature. Thus, the radical anion, $[Fe(NO)_2PR_3(\eta^2\text{-TCNE})]^-$, decomposes rapidly to yield a decomposition product, **P**. The irreversible oxidation peak observed at much higher potential relative to the reduction, listed as $E_{pa}(P)$ in Table 4, is attributable specifically to the oxidation of the product **P**. This was confirmed by the absence of this peak

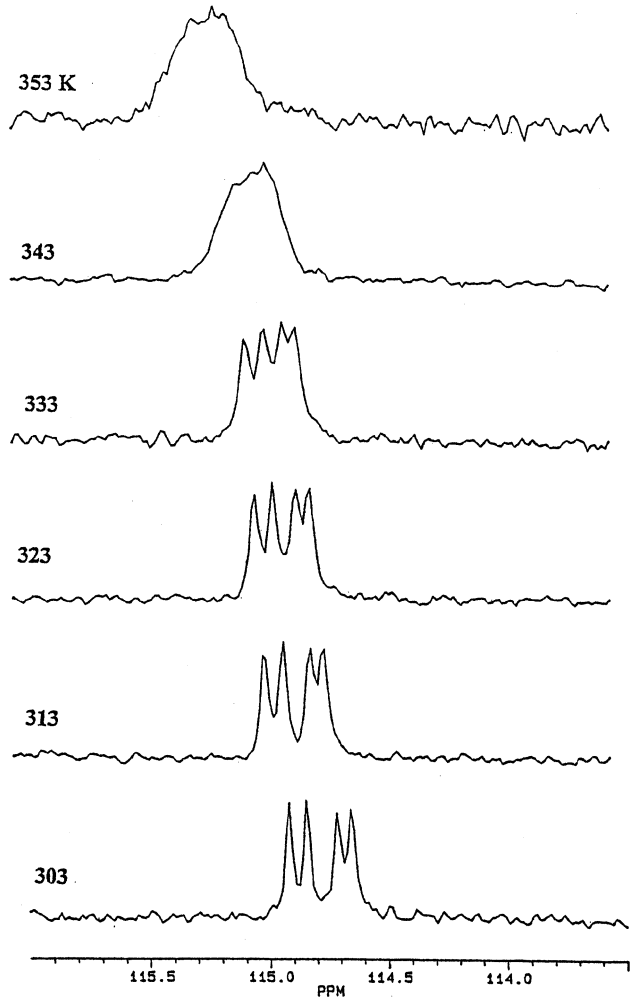

FIGURE 8 Variable-temperature ^{13}C NMR spectra of **3** recorded a Bruker AC 300 operating at 75.47 MHz at a magnetic field strength of 7.05 Tesla in CD_3CN. Reprinted from ref. 29. Copyright (1998), with permission from Elsevier Science.

when the potential was switched off before the potential required to reduce **3–6** (the potential range was set from 0.50 V to -0.96 V for **3**; and 0.50 V to -1.12 V for **4–6**) was reached.

The complexes **3, 4, 5,** and **6** ($E_{pc} = -0.990$ V ~ -1.146 V) are harder to reduce than the free TCNE ligand ($E_{1/2} = -0.207$ V), but are easier to

TABLE 4 Electrochemical Potentials of Iron Dinitrosyl Complexes *vs.* $FeCp_2^+/FeCp_2$ at Scan Rate of 100 mV/s and the pK_a Values for the Phosphines and Phosphite

Complexes	NO stretch(es) (cm^{-1})[b]	NO stretches (Average) (cm^{-1})	E_{pc} (V)	E_{pa}(P) (V)	$E°(\Delta E)$[a] (V)	pK_a (Phosphine)[49]
$Fe(NO)_2[P(OMe)_3]$ (η^2-TCNE), **3**	1843, 1797	1820	−0.990	−0.398		2.6
$Fe(NO)_2[PEt_2Ph]$ (η^2-TCNE), **6**	1827; 1790	1808.5	−1.120	−0.604		6.25
$Fe(NO)_2[PMe_2Ph]$ (η^2-TCNE), **5**	1830; 1786	1808	−1.123	−0.607		6.5
$Fe(NO)_2[P(n\text{-}Bu)_3]$ (η^2-TCNE), **4**	1824; 1785	1804.5	−1.146	−0.652		8.43
$Fe(NO)_2[P(OMe_3)](CO)$	1770; 1722	1746			−1.96 (125 mV)	2.6
$Fe(NO)_2[PEt_2Ph](CO)$	1755; 1706	1730.5			−2.108 (131 mV)	6.25
$Fe(NO)_2[PMe_2Ph](CO)$	1754; 1708	1731			−2.101 (268 mV)	6.5
$Fe(NO)_2[P(n\text{-}Bu)_3](CO)$	1752; 1704	1728			−2.150 (130 mV)	8.43

[a]These are one electron reductions by comparison with equimolar ferrocene oxidation reactions.
[b]The numbers shown were measured in CH_2Cl_2 solution.

reduce than the corresponding carbonyl compound, $Fe(NO)_2(PR_3)(CO)$ ($E^\circ = -1.96 \sim -2.15$ V). The coordination of TCNE leads to a shift in the reduction potentials to a more negative value compared to free TCNE, and to a more positive value in comparison to $Fe(NO)_2(PR_3)(CO)$. This indicates that the back-bonding from the iron center to the TCNE ligand is stronger than the characteristic covalent bonding arising from σ-donation by the TCNE ligand. This back-donation to the TCNE ligand renders the iron atom partially positive, and thereby easier to reduce. The reduction is presumed to occur at the iron center rather than on the TCNE ligand since the basicity of the phosphorus moiety has an impact on the electrochemical behavior of these compounds. Upon evaluation of the data presented in Table 4, it is apparent that a cathodic shift in potential for both the E° values and the E_{pc} and $E_{pa}(P)$ values occurs for an increase in the phosphine or phosphite pK_a. This observation can be qualitatively rationalized in that with increasing electron density being donated to the iron center, it is rendered less prone to reduction. It is well established that, in transition metal carbonyl complexes, the carbonyl stretching frequencies are a good reflection of the phosphine donating or withdrawing character. However, a correlation between the pK_a values and reduction potentials has recently been observed for a series of phosphine-substituted metal carbonyls.[51] Table 4 also lists the averaged IR stretching frequencies for the nitrosyls, which demonstrates the trend of decreasing IR frequencies with increasing pK_a values.

CONCLUSIONS

We have demonstrated that iron nitrosyl complexes interact with imidazole based ligands to yield "g = 2.03" radicals and **1** was fully characterized by NMR, IR, MS and X-ray crystallography. These findings challenge biological chemists to determine whether the radicals they observe at g = 2.03 could be not only iron nitrosyl with thiols or cysteine residue, but also iron nitrosyl attached to other amino acids of proteins. Further studies are underway to isolate other g = 2.03 species and to establish the structures in biological systems containing nitrosyl non-heme-iron and amino acids of proteins.

The reactions of $Fe(NO)_2(CO)(PR_3)$ with TCNE yield η^2-coordinated TCNE to iron dinitrosyls. The formation of these complexes is well explained by an electron transfer autocatalysis mechanism. X-ray crystallographic studies on **2** and **3** show the iron to be situated in a nearly tetrahedral environment with a π-bonded tetracyanoethylene and two linearly bound nitrosyl groups. From the ambient-temperature NMR spectral data, it is evident that there exist two non-equivalent cyanocarbon environments, indicating that the rotation about the Fe-TCNE π-bond is slowed at room temperature. Variable-temperature NMR studies on $Fe(NO)_2[P(OMe)_3](\eta^2\text{-TCNE})$ yielded an activation energy barrier of

approximately 18.1 ± 0.5 kcal/mol for this rotational process. Electrochemical studies revealed that the neutral $Fe(NO)_2[PR_3](\eta^2\text{-TCNE})$ complexes undergo irreversible reductions at positively shifted potentials, relative to the related $Fe(NO)_2[PR_3](CO)$ complexes. Moreover, a trend toward cathodic shift of the reduction potentials with increasing phosphine pK_a has been observed. The high energy barrier for alkene rotation and the shift towards positive reduction potentials are rationalized in terms of a strong π-interaction between the iron center and TCNE.

ACKNOWLEDGMENTS

This work was supported in part by the Natural Sciences and Engineering Research Council of Canada, National Institute of Health – MBRS SCORE Program (Grant # 1 S06 GM63119-01), Research Corporation (Grant # CC5392) and American Chemical Society-Petroleum Research Fund (Grant # 37034-GB3).

REFERENCES

1. Feldman, P. L., Griffith, O. W., Stuehr, D. J. 1993. *Chem. Eng. News*, Dec. 20, 26.
2. Legzdins, P., Richter-Addo, G. B., Burstyn, J. 2002. *Chem. Rev*., 102, Issue 4.
3. Lancaster, Jr., J. R., Hibbs, Jr., J. B. 1990. *Proc. Natl. Acad. Sci. USA*, 87, 1223–1227.
4. Vanin, A. F., Varich, V. Y. 1981. *Stud. Biophys.*, 86, 177–179.
5. Muller, B., Kleschyov, A. L., Stoclet, J. C. 1996. *Brit. J. Pharm.*, 119, 1281–1285.
6. Vanin, A. F. 1991. *FEBS Lett*., 289, 1–3.
7. Butler, A. R., Flitney, F. W., Williams, D. L. H. 1995. *Trends Pharmacol. Sci.*, 16, 18–22.
8. Noguchi, T., Honda, J., Nagamune, T., Sasabe, H., Inoue, Y., Endo, I. 1995. *FEBS Lett*., 358, 9–12.
9. Lee, M., Arosio, P., Cozzi, A., Chasteen, N. D. 1994. *Biochem.*, 33, 3679–3687.
10. Drapier, J. C., Pellat, C., Henry Y. 1991. *J. Biol. Chem.*, 266, 10162–10167.
11. McDonald, C. C., Phillips, W. D., Mower, H. F. 1965. *J. Am. Chem. Soc.*, 87, 3319–3326.
12. Woolum, J. C., Tiezzi, E., Commoner, B. 1968. *Biochim. Biophys. Acta*, 160, 311–320.
13. Basolo, F. 1990. *Polyhedron*, 9, 1503–1535.
14. Butler, A. R., Glidewell, C., Li, M. 1988. *Adv. Inorg. Chem*., 32, 335–393.
15. Dieck, H. T., Bruder, H., Kuhl, E., Junghans, D., Hellfeldt, K. 1989. *New J. Chem*., 13, 259–268.
16. Chong, K. S., Rettig, S. J., Storr, A., Trotter, J. 1979. *Can. J. Chem.*, 57, 3119–3125.
17. Rettig, S. J., Storr, A., Summers, D. A., Thompson, R. C., Trotter, J. 1997. *J. Am. Chem. Soc.*, 119, 8675–8680.
18. Hagadorn, J. R., Que, L., Jr., Tolman, W. B. 1998. *J. Am. Chem. Soc.*, 120, 13531–13532.
19. Candlin, J. P., Janes, W. H. 1968. *J. Chem. Soc. C*, 1856.
20. Ballivet-Tkatchenko, D., Riveccie, M., El-Murr, N. 1979. *J. Am. Chem. Soc.*, 101, 2763.
21. Ballivet-Tkatchenko, D., Billard, C., Revillon, A. 1981. *J. Polym. Sci.*, 19, 1697.
22. Gadd, G. E., Poliakoff, M., Turner, J. J. 1987. *Organometallics*, 6, 391.

23. Ballivet-Tkatchenko, D., Vincent-Vaucquelin, J., Nickel, B., Rassat, A. 1989. *Paramagnetic Organometallic Species in Activation/Selectivity Catalysis*, M. Chanon, M. Julliard and J. C. Poite, eds. New York, Kluwer Academic Publishers, p. 61.
24. Bryar, T. R., Eaton, D. R. 1992. *Can. J. Chem*., 70, 1917.
25. Atkinson, F. L., Blackwell, H. E., Brown, N. C., Connelly, N. G., Crossley, J. G., Orpen, A. G., Rieger, A. L., Rieger, P. H. 1996. *J. Chem. Soc. Dalton Trans*., 3491.
26. Wah, H. L. K., Postel, M., Tomi, F. 1989. *Inorg. Chem*., 28, 233.
27. Wah, H. L. K., Postel, M., Tomi, F., Agbossou, F., Ballivet-Tkatchenko, D., Urso, F. 1993. *Inorg. Chim. Acta*, 205, 113.
28. Li, L., Enright, G. D., Preston, K. F. 1994. *Organometallics*, 13, 4686–4688.
29. Hörsken, A., Zheng, G., Stradiotto, M., McCrory, C. T. C., Li, L. 1998. *J. Organomet. Chem.*, 558, 1–9.
30. Li, L., Morton, J. R., Preston, K. F. 1995. *Mag. Res. Chem*., 33, S14–S19.
31. Reginato, N., McCrory, C. T. C., Pervitsky, D., Li, L. 1999. *J. Am. Chem. Soc*., 121, 10217–10218.
32. Enemark, J. H., Feltham, R. D. 1974. *Coord. Chem. Rev.*, 13, 339–406.
33. Sezowska-Trzebiatowska, B., Jezierski, A., Kozlowski, A. 1972. *Bull. Acad. Pol. Sci. Ser. Sci. Chim.*, 20, 249–253.
34. The MO calculation was done at the Extended Hδckel level using the program of CACAO (Mealli, C., Proserpio, D. M. 1990. *J. Chem. Edu*. 67, 3399). The positional coordinates of **1** were obtained from the X-ray crystal structure parameters.
35. Allano, V. G., Araneo, A., Bellon, P. L., Ciani, G., Manassero, M. 1974. *J. Organomet. Chem*., 67, 413.
36. Morris, D. E., Basolo, F. 1968. *J. Am. Chem. Soc*., 90, 2531.
37. Therien, M. J., Ni, C. L., Anson, F. C., Osteryoung, J. G., Trogler, W. C. 1986. *J. Am. Chem. Soc.*, 108, 4037.
38. Liaw, W. F., Chiang, C. Y., Lee, G. H., Peng, S. M., Lai, C. H., Darensbourg, M. Y. 2000. *Inorg. Chem*., 39, 480.
39. Rosenblum, M., Fish, R. W., Bennet, C. 1964. *J. Am. Chem. Soc.*, 86, 5166.
40. (a) Rettig, M. F., Wing, R. W. 1969. *Inorg. Chem.*, 8, 2685.
    (b) Olbrich-Deubner, B., Grob, V., Kaim, W. 1989. *J. Organomet. Chem.*, 366, 155.
41. Richter-Addo, G. B., Legzdins, P. 1992. *Metal Nitrosyls*. New York, Oxford University Press, p. 81.
42. Mingos, D. M. P. 1982. *Comprehensive Organometallic Chemistry*, Vol. 3, 1.
43. Stradiotto, M., Britten, J. F., Li, L. Personal Communication.
44. McGinnety, J. A., Ibers, J. A. 1968. *Chem. Commun.*, 235.
45. Green, M., Osborn, R. B. L., Rest, A. J., Stone, F. G. A. 1966. *Chem. Commun.*, 502.
46. Cramer, R., Kling, J. B., Roberts, J. D. 1969. *J. Am. Chem. Soc.*, 91, 2519.
47. Jackman, J. M., Cotton, F. A. 1975. *Dynamic Nuclear Magnetic Resonance Spectroscopy.* New York: Academic Press.
48. Kaneshima, T., Kawakami, K., Tanaka, T. 1974. *Inorg. Chem.*, 13, 2198.
49. Kawakami, K., Kaneshima, T., Tanaka, V. 1972. *J. Organomet. Chem.*, 34, C21.
50. Wheelock, K. S., Nelson, K. S., Cusachs, L. C., Jonassen, H. B. 1970. *J. Am. Chem. Soc.*, 92, 5110.
51. Rahman, M. M., Liu, H.-Y., Eriks, K., Prock, A., Giering, W. P. 1989. *Organometallics*, 8, 1 and references cited within.